We are IntechOpen, the world's leading publisher of Open Access books Built by scientists, for scientists

4,800
Open access books available

122,000
International authors and editors

135M
Downloads

Our authors are among the

154
Countries delivered to

TOP 1%
most cited scientists

12.2%
Contributors from top 500 universities

WEB OF SCIENCE™

Selection of our books indexed in the Book Citation Index in Web of Science™ Core Collection (BKCI)

Interested in publishing with us?
Contact book.department@intechopen.com

Numbers displayed above are based on latest data collected.
For more information visit www.intechopen.com

12

Contribution to the Evaluation of Silicon Carbide Surge Arresters

Arnaldo Gakiya Kanashiro and Milton Zanotti Jr.
University of São Paulo
Brazil

1. Introduction

Basically, there are two types of surge arresters installed in the power system: the silicon carbide (SiC) surge arresters and the zinc oxide (ZnO) ones. The SiC surge arresters are being replaced by the latter but a large number are still operating in the electrical system. Due to high costs and operational difficulties it is not possible to replace all the SiC surge arresters in a short term and the utilities have to manage both technologies (Carneiro, 2000). Therefore, in order to avoid failure, it is very important to know the level of degradation of the SiC surge arresters, most of them with 20 or more years of service. The diagnostic techniques applied to the ZnO surge arresters have been developed for many years and they are presented in (Heinrich & Hinrichsen, 2001) and (Kannus & Lahti, 2005). The main techniques are: thermovision and leakage current measurement. The leakage current measurement can give valuable information about the degradation of the ZnO surge arresters. The level of degradation is proportional to the magnitude of the resistive component of the total leakage current. Regarding the SiC surge arresters, there is no recommendation according to the (IEC-60099-5, 2000) standard.

This chapter is focused on the application of the leakage current aiming the diagnostic of the SiC surge arresters. In the electrical utilities, the thermovision technique is also applied to the SiC surge arresters but it is very difficult to conclude, among several arresters, which of them are more degraded in order to replace them and to avoid failure (Almeida et al., 2009). This chapter describes the methodology and the results of the investigation that was performed aiming the application of the leakage current technique to the SiC surge arresters. The basic idea was to correlate the level of degradation of the SiC surge arresters with the magnitude of the third harmonic (3^a H) of the total leakage current. Laboratory tests were performed in arresters that had been replaced in the substations. The characteristics of the leakage current showed a good correlation with the degradation of the arresters. Some of them were disassembled in order to verify their internal components. Afterwards, measurements were carried out in substation aiming to verify the feasibility of the technique in the field. Another substation was also evaluated, and based on the leakage current measurements obtained some SiC arresters were replaced. The results obtained in the investigation might help the utilities to develop more adequate maintenance programs.

2. Methodology

The methodology of the investigation was based on laboratory tests and visual inspection of the internal components of the surge arresters (Kanashiro et al., 2009). The first step of the research was to analyze the characteristics of the SiC surge arresters in service, considering their age, manufacturer, rated voltage, etc. Then, some arresters were selected to be tested at the laboratory, considering the nominal voltages of 88 kV, 138 kV, 230 kV, 345 kV and 440 kV, from five manufacturers. These SiC surge arresters were no longer being used by the utility in its electrical system because they were either replaced by ZnO surge arresters or presented abnormal heating during thermovision periodical measurements.

The surge arresters operated during about 20 up to 25 years in the electrical system; however, there wasn't any information about their behaviour during this time period. Therefore, the values of the power frequency spark-over voltage and lightning spark-over voltage tests, obtained at the laboratory, were firstly used as reference to indicate degradation, taking into account the requirements of the manufacturers and of the (IEC 60099-1, 1999) standard.

Afterwards, measurements of the leakage current were carried out, with the amplitude (I_{peak}) and the 3ª H component being obtained. The phase difference between the leakage current and the voltage applied to the surge arrester was also determined. Then, radio influence voltage (RIV) tests, with frequency of 500 kHz and impedance of 300 Ω, and thermovision measurements were also performed for some selected arresters.

In some of the 88 kV arresters, surface erosion was observed which is a typical sign of electric arc damage on the porcelain, as shown in Fig. 1. Also, most of them had some degree of corrosion in their metallic parts, as shown in Fig. 2. Finally, in order to check the viability of measuring the leakage current in the field, some SiC surge arresters installed at Paraibuna substation were chosen. After this, due to the explosion of one 88 kV SiC surge arrester at Mairiporã substation, leakage current measurements were also performed in this substation.

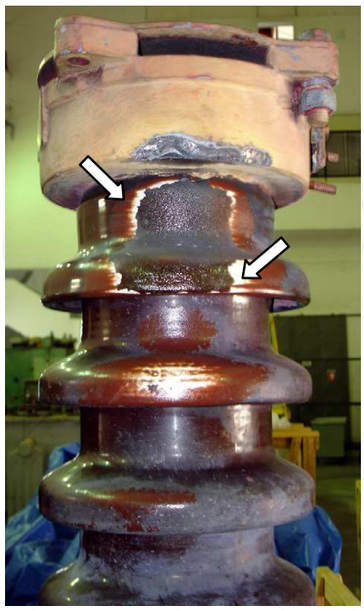

Fig. 1. Typical sign of electric arc damage on the porcelain of the surge arrester.

Fig. 2. Corrosion in the metallic parts of the surge arrester.

In the next section, the main results of the investigation, related to the diagnostic of the SiC surge arresters, are presented. The results refer to the 88 and 138 kV surge arresters.

3. Results and Discussion

3.1 Laboratory tests

Because some of the SiC surge arresters presented signs of electric arc damage on the porcelain and, also, corrosion in their metallic parts, prior to the laboratory tests, measurements of insulation resistance and of Watts losses, were carried out on several samples, aiming at a preliminary check of their general condition. The results of the power frequency spark-over voltage and lightning spark-over voltage tests are shown in Table 1 and Table 2. According to the manufacturer's requirements, all 88 kV samples failed the power frequency spark-over voltage test. In this test, samples A5 and A6 presented unstable behaviour.

The 138 kV samples A7, A8, A9, C5, D3 and D5 failed the power frequency spark-over voltage test. Regarding the lightning spark-over voltage test, all samples (88 kV and 138 kV) fulfilled the manufacturer's requirements.

Manufacturer A	Power frequency spark-over voltage (kV)	Lightning spark-over voltage (kV)	
		Positive	Negative
A1	134	182	181
A2	105	171	168
A3	85	178	178
A4	102	172	167
A5	-----	173	172
A6	-----	173	188

Table 1. 88 kV surge arresters.

Manufacturers A/B/C/D	Power frequency spark-over voltage (kV)	Lightning spark-over voltage (kV)	
		Positive	Negative
A7	193	227	227
A8	170	222	228
A9	178	225	224
B1	244	284	272
B2	246	279	272
B3	242	287	294
B4	233	234	225
B5	237	234	229
B6	241	271	269
B7	232	272	272
C1	226	382	354
C2	219	374	363
C3	224	364	359
C4	218	340	322
C5	188	349	344
C6	233	355	344
D1	274	374	367
D2	273	376	372
D3	268	376	366
D4	271	372	369
D5	262	378	369

Table 2. 138 kV surge arresters.

Afterwards, measurements of the total leakage current were carried out, with the I_{peak} values and the 3^a H component being obtained. The phase difference between the total leakage current and the voltage applied to the sample was also determined. The results, with the exclusion of samples A5 and A6, are shown in Table 3.

Manufacturers A/B/C/D	Power frequency spark-over voltage (kV)	Leakage current		Phase difference (degree)
		I_{peak} (mA)	3ª H (%)	
A1	134 (F)	0.172	6.7	89
A2	105 (F)	0.192	10.1	65
A3	85 (F)	0.412	24.9	54
A4	102 (F)	0.696	32.9	47
A7	193 (F)	0.278	2.6	85
A8	170 (F)	0.268	5.6	70
A9	178 (F)	0.246	6.8	71
B1	244	0.226	4.8	72
B2	246	0.252	5.7	70
B3	242	0.370	6.0	77
B4	233	0.234	6.4	68
B5	237	0.251	6.8	68
B6	241	0.230	8.5	63
B7	232	0.261	9.4	53
C1	226	0.363	5.6	73
C2	219	0.456	5.8	75
C3	224	0.346	6.8	79
C4	218	0.332	6.9	68
C5	188 (F)	0.430	7.5	83
C6	233	0.726	18	51
D1	274	0.364	1.9	89
D2	273	0.357	2.1	89
D3	268 (F)	0.357	2.1	82
D4	271	0.330	2.5	84
D5	262 (F)	0.331	3.8	78

Table 3. Leakage current measurement.

In Table 3, (F) means that the sample failed the power frequency spark-over voltage test. After the measurements above, some arresters were selected to be submitted to the radio influence voltage (RIV) and thermovision tests.
In the three tests, leakage current, RIV and thermovision, the phase-to-ground voltages 51 kV and 80 kV were applied to the 88 kV and 138 kV samples, respectively.
The thermovision were carried out after the samples had been energised for a time period of 5 to 7.5 hours, depending on the manufacturer. One measurement was carried out for each of four different sides of the sample. Each measurement corresponds to the thermal imaging obtained along the sample, from top to bottom. Each of the four sides of the sample had its maximum and minimum temperatures determined, and the difference (Δt) between these temperatures was calculated. The greatest difference value found was named "Δt_{max}".
The highest temperature value obtained in the sample was named "t_{max}". The results are shown in Table 4, where (F) means that the sample failed the power frequency spark-over voltage test, (*) means that significant results were not observed in the RIV test and (**) that the sample was not tested. Fig. 3 shows an example of a thermal image measurement.

Surge arresters	Leakage current		RIV (μV)	Thermovision (^{0}C)	
	I_{peak} (mA)	3ª H (%)		t_{max}	Δt_{max}
A1	0.172	6.7	< 25	20.8	2.0
A2	0.213	10.1	*	21.6	2.0
B2	0.252	5.7	< 25	28.0	4.6
B3	0.370	6.0	*	28.3	4.3
B6	0.230	8.5	< 25	27.9	4.4
C3	0.346	6.8	< 25	19.9	2.6
C5 (F)	0.430	7.5	4518	19.3	2.8
C6	0.726	18	6381	32.6	17.6
D1	0.364	1.9	< 25	18.1	1.7
D3 (F)	0.357	2.1	64	18.2	1.9

Table 4. Results of the leakage current measurement, RIV and thermovision.

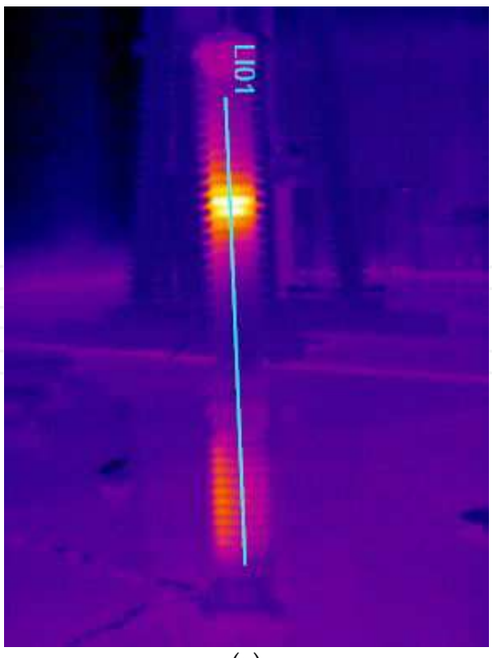

(a)

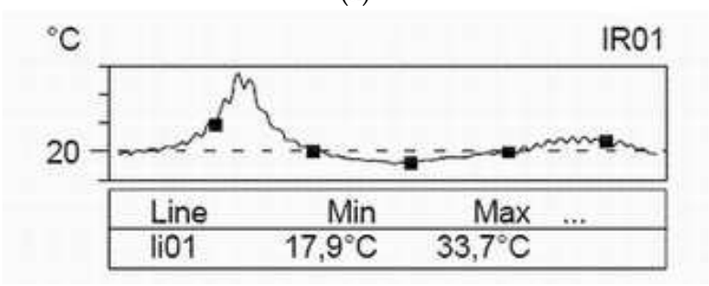

(b)

Fig. 3. Example of a thermal image measurement, (a) thermal image of the surge arrester and (b) temperature along the surge arrester.

The following aspects can be pointed out, concerning the results shown in Table 3 and Table 4:

Manufacturer A - 88 kV surge arresters:

- all surge arresters failed the power frequency spark-over voltage test;
- surge arrester A1 presented the highest power frequency spark-over voltage value (134 kV), the lowest amplitude value of the leakage current (0.172 mA), the lowest 3^a H component (6.7 %) and the greatest phase difference (89^0);
- on the other hand, surge arrester A4, which showed the greatest amplitude of the leakage current (0.696 mA), had the greatest 3^a H component (32.9 %) and the lowest phase difference (47^0).

Manufacturer A – 138 kV surge arresters:

- all surge arresters failed the power frequency spark-over voltage test;
- surge arrester A7, which presented the highest power frequency spark-over voltage value (193 kV), also had the lowest harmonic distortion (2.6 %) and the greatest phase difference (85^0);

- significant results were not observed in the RIV and thermovision measurements.

Manufacturer B – 138 kV surge arresters:
- all surge arresters were successful in the power frequency spark-over voltage tests;
- surge arresters B6 and B7 presented harmonic distortion values (8.5 % and 9.4 %, respectively) greater than the values obtained with other samples of the same manufacturer. Smaller phase difference values were also obtained (63^0 and 53^0, respectively);
- significant results were not obtained in the RIV and thermo vision measurements.

Manufacturer C – 138 kV surge arresters:
- surge arrester C5 failed the power frequency spark-over voltage test and presented 3^a H component of 7.5 % and phase difference of 83^0;
- although surge arrester C6 was succesful in the power frequency spark-over voltage test, it presented leakage current amplitude of 0.726 mA, distortion of 18 % and phase difference of 51^0, which may indicate some degradation of its internal components;
- surge arresters C5 and C6 had high RIV values, suggesting the presence of internal electrical discharges. In spite of this, the thermovision measurement showed higher temperature only in surge arrester C6.

Manufacturer D – 138 kV surge arresters:
- surge arresters D3 and D5 failed the power frequency spark-over voltage test;
- surge arrester D5, which presented the lowest power frequency spark-over voltage value, had the greatest leakage current distortion (3.8 %) and the smallest phase difference (78^0);
- significant results were not observed in the RIV and thermovision measurements.

3.2 Internal components of the surge arresters

Some of the surge arresters were disassembled in order to verify the correlation between the presence of deterioration in their internal parts and the results obtained in the laboratory tests. The following surge arresters were selected: A2, A4, A6 (manufacturer A) and C1, C3 and C5 (manufacturer C).

In the surge arresters A2, A4 and A6 there are permanent magnets in parallel with gap electrodes. Nonlinear resistors of SiC are placed between the gap electrodes. The dismantled surge arrester of manufacturer A can be seen in the Fig. 4.

In the SiC surge arresters of manufacturer C, the gap electrodes are divided in groups. In each group a tape is applied to fix the gap electrodes. A nonlinear resistor is placed in parallel with each group to equalize the voltage potential of the gap electrodes.

The internal components of the surge arrester C can be seen in Fig. 5. At the edges are placed coils in order to facilitate arc extinguishing. Fig. 6 shows one group of gap electrodes.

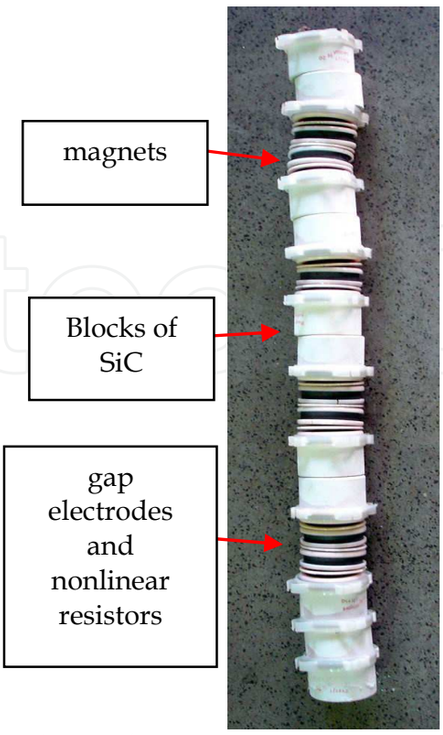

Fig. 4. Surge arrester of manufacturer A.

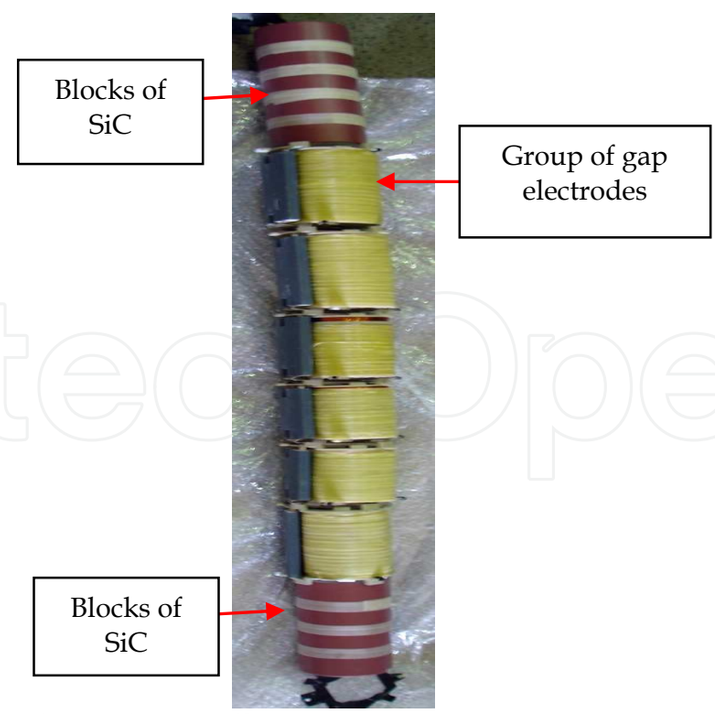

Fig. 5. Surge arrester of manufacturer C.

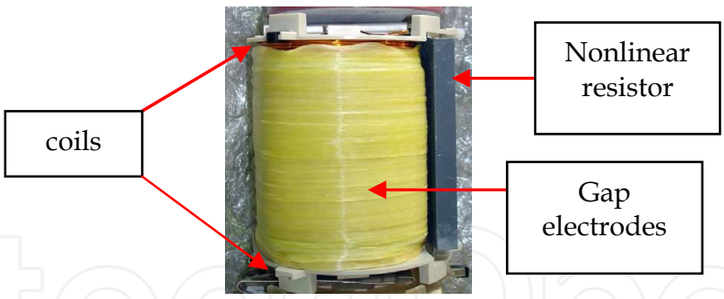

Fig. 6. Group of gap electrodes of surge arrester C.

In general, it was noticed that moisture was presented in the internal components of the arresters. Some traces of discharges on the surface of the blocks were also observed. Some of the surge arresters presented signs of discharges in the gap electrodes. During the visual inspection, it was also observed that some nonlinear resistors were damaged.
The surge arrester A6 (manufacturer A) was more degraded in comparison with A2 and A4. The arrester C5 (manufacturer C) was the worst in comparison to the surge arresters C1 and C3.
The surge arrester C5 presented some damaged nonlinear resistors and, probably, this was the reason for the high level of RIV (4,518 μV), shown in Table 4. This surge arrester also failed the power frequency spark-over voltage test. In Fig. 7 and Fig. 8 it is possible to visualize the condition of the components of the surge arresters, considering manufacturers A and C, respectively.
As a general conclusion, it was observed that the surge arresters of manufacturers A and C presented evidence of ingress of moisture and signs of discharges. Moisture ingress may have deteriorated the SiC material (McDermid, 2002) and (Grzybowski, 1999).
Afterwards, surge arresters of manufacturer B were also dismantled and it was observed that the internal components were in good condition. These results mean that they could have remained in service until they needed to be replaced by the ZnO surge arresters.
After disassembling the surge arresters, the following aspects can be pointed out, concerning the results shown in Table 3 and Table 4:
- the highest values of the leakage current, in terms of amplitude and harmonic distortion, corresponded to the degradation of the surge arresters;
- the thermovision technique, RIV tests and also the leakage current, considering the C6 sample, showed that this surge arrester was degraded. The visual inspection of its internal components confirmed this assumption;
- the surge arresters C5 presented high RIV values, suggesting the presence of internal electrical discharges. In spite of this, the thermovision measurement showed higher temperature only in surge arrester C6;
- the B1 to B7 surge arresters were successful in all tests but samples B6 and B7 presented greater harmonic distortion values and should be removed first from the electrical system;
- the leakage current values, in terms of the amplitude and the third harmonic component, could be used to select the SiC surge arresters to be replaced by the ZnO ones.

(a)

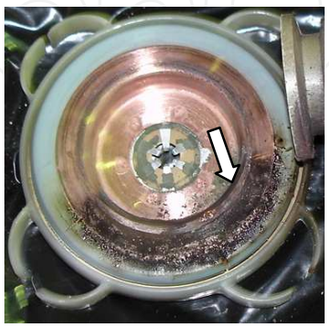

(b)

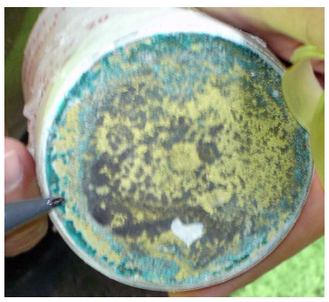

(c)

(d)

Fig. 7. Surge arresters of manufacturer A, (a) blocks: signs of discharge, (b) gap electrodes: signs of discharge, (c) block: presence of moisture and (d) gap electrode: signs of discharge.

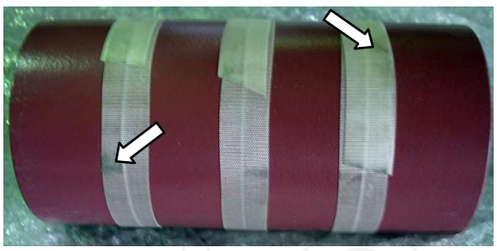

(a)

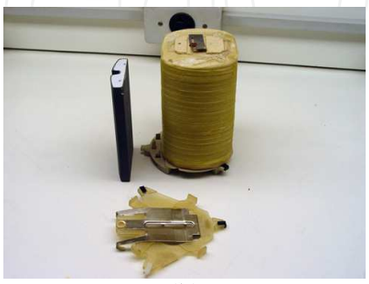

(b)

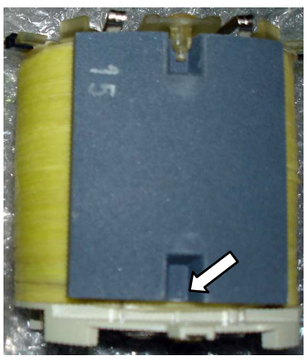

(c)

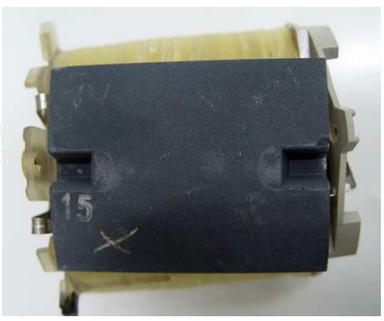

(d)

Fig. 8. Surge arresters of manufacturer C, (a) block surface: presence of moisture, (b) group of gap electrodes: damaged, (c) nonlinear resistor: broken and (d) nonlinear resistor: broken.

4. Measurements at Substation

Leakage current measurements in 88 kV SiC surge arresters, in service, were performed in the Paraibuna substation first, aiming to check the viability of this technique. Details of the SiC surge arresters installation were considered, such as presence of counter discharges, grounding cable of the surge arresters, the presence of insulators in the assembled surge arresters, etc. These aspects have important influence on the results. A device, consisting of a current transformer (CT) and a digital instrument, was used in the field. The CT was placed in the grounding cable, between the discharges counter and the bottom part of the surge arrester (position 1) or after the discharge counter (position 2), as shown in Fig. 9. The aim was to investigate the interference of the installation in the results. The leakage current was measured using 60 Hz and 180 Hz frequencies. When the CT was placed in the position 2, there was interference, as shown in the oscillograms of Fig. 10.

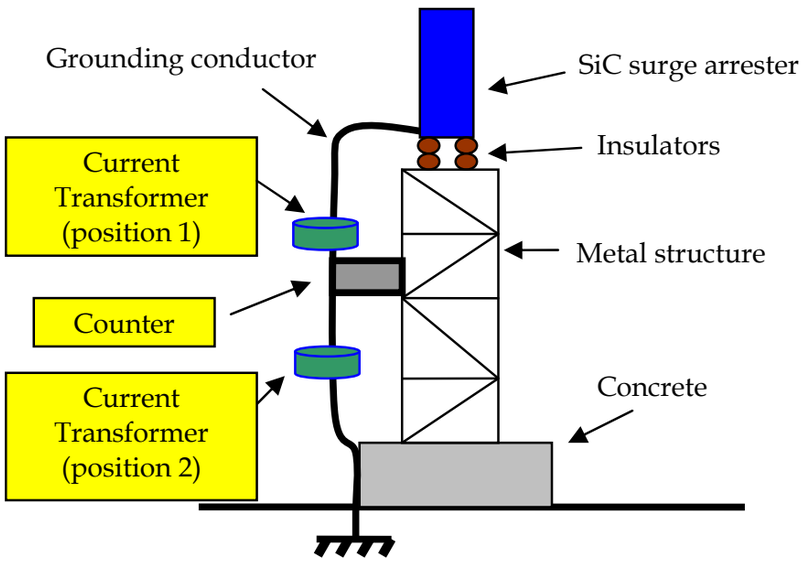

Fig. 9. Leakage current measurement at the substation.

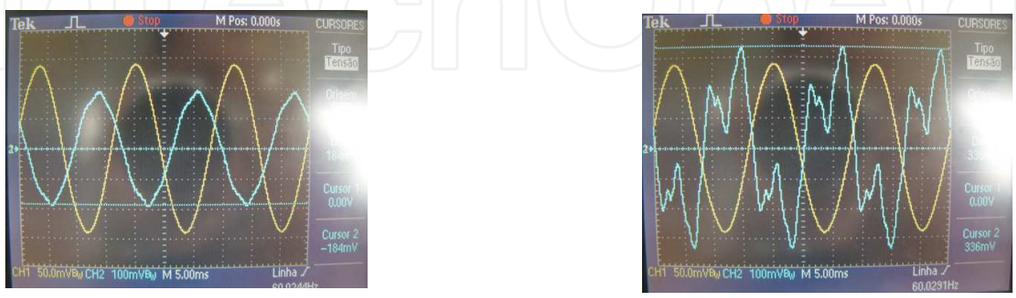

(a) (b)

Fig. 10. Waveforms of the leakage current (blue) and of the applied voltage (yellow), (a) CT in the position 1 and (b) CT in the position 2.

The SiC surge arresters were installed in the 88 kV, circuits TAU-01, JAG-01 and JAG-02. The three phases of each circuit were named as a, b and c. Table 5 shows the results. The comparison between the results from the field and from the laboratory is not so easy because the manufacturers of the surge arresters are not the same, therefore, it is possible to observe that the values are relatively low.

Surge arresters	Leakage current 60 Hz rms (mA)	Leakage current 180 Hz rms (mA)
TAU-01a	0.132	0.005
TAU-01b	0.128	0.004
TAU-01c	0.112	0.004
JAG-01a	0.170	0.004
JAG-01b	0.078	0.002
JAG-01c	0.163	0.005
JAG-02a	0.122	0.003
JAG-02b	0.088	0.002
JAG-02c	0.070	0.002

Table 5. 88 kV arresters – Paraibuna substation.

Afterwards, due to the explosion of one 88 kV SiC surge arrester at Mairiporã substation, several measurements of the leakage current were performed in that substation. 88 kV and 138 kV SiC surge arresters in service, were measured and the results are presented in Table 6 and Table 7, respectively.

Surge arresters	Leakage current 60 Hz rms (mA)	Leakage current 180 Hz rms (mA)
JAG-2a	0.182	0.013
JAG-2b	0.126	0.011
JAG-2c	0.124	0.013
JAG-1a	0.078	0.010
JAG-1b	0.092	0.014
JAG-1c	0.281	0.055

Table 6. 88 kV arresters – Mairiporã substation.

Surge arresters	Leakage current 60 Hz rms (mA)	Leakage current 180 Hz rms (mA)
BRP-1a	0.122	0.011
BRP-1b	0.096	0.012
BRP-1c	0.114	0.013
BRP-2a	0.089	0.009
BRP-2b	0.092	0.009
BRP-2c	0.102	0.009
SAA-1a	0.110	0.011
SAA-1b	0.079	0.010
SAA-1c	0.088	0.011
SAA-2a	0.083	0.008
SAA-2b	0.070	0.009
SAA-2c	0.055	0.009
CAV-1a	0.095	0.005
CAV-1b	0.061	0.012
CAV-1c	0.100	0.007
CAV-2a	0.082	0.006
CAV-2b	0.075	0.006
CAV-2c	0.076	0.007
SAI-1a	0.085	0.002
SAI-1b	*	*
SAI-1c	0.145	0.005
SAI-2a	0.143	0.004
SAI-2b	*	*
SAI-2c	0.161	0.005

Table 7. 138 kV arresters – Mairiporã substation.

It can be observed in Table 6 that the surge arrester, installed in the circuit JAG-1c, presented high values of leakage current and, probably, the degradation of its internal components is higher than the other arresters of the same circuit. Then, the arresters were removed from the substation. The thermovision measurements, uncluding the surge arresters of the circuit

(JAG-1a, JAG-1b, JAG-1c) indicated heating in the surge arresters JAG-1b and JAG-1c. In Table 7, the leakage current measurement was not performed in the surge arresters of the circuits SAI-1b and SAI-2b. All the surge arresters were made by the same manufacturer, except the arresters of the circuit SAI-1 and SAI-2. The leakage current values are low and the thermovision measurements did not indicate heating in the surge arresters. The RIV test is very difficult to apply in the field, then, in Mairiporã substation, measurements of the conducted electromagnetic field, generated by partial discharges, were performed. The aim was to identify the SiC surge arresters with internal electrical discharges.

5. Conclusion

This chapter shows results of laboratory tests and substations measurements concerning the diagnostic of the 88 kV and 138 kV SiC surge arresters. The results showed that the leakage current measurement, one of the techniques used to evaluate the ZnO surge arresters, can also be used to assess the SiC surge arresters, having obtained important information about their condition. This conclusion might help the electrical utilities to develop more adequate maintenance programs and to more accurately select the SiC surge arresters that need replacement in the substations.

6. References

Almeida, C. A. L., Braga, A. P., Nascimento, S., Paiva, V., Martins, H. J. A., Torres, R. & Caminhas, W. M. (2009). Intelligent thermographic diagnostic applied to surge arresters: a new approach. *IEEE Transactions on Power Delivery*, Vol. 24, No. 2, (April 2009) 751-757, ISSN 0885-8977.

Carneiro, J. C. (2007). Policy for renewal of power system substations silicon carbide (SiC) surge arresters: a new technical economical vision, *Proceedings of the IX International Symposium on Lightning Protection (IX SIPDA),* pp. 294–299, ISSN 2176-2759, Foz do Iguaçu, September 2007, IEE/USP, São Paulo.

Grzybowski, S. & Gao, G. (1999). Evaluation of 15-420 kV substation lightning arresters after 25 years of service, *Proceedings of the IEEE Southeastcon'99,* pp. 333–336, ISBN 0-7803-5237-8, Lexington, March 1999.

Heinrich, C. & Hinrichsen, V. (2001). Diagnostics and monitoring of metal-oxide surge arresters in high-voltage – comparison of existing and newly developed procedures. *IEEE Transactions on Power Delivery*, Vol. 16, No. 1, (January 2001) 138-143, ISSN 0885-8977.

Kanashiro, A. G., Zanotti Junior, M., Obase, P. F. & Bacega, W. R. (2009). Diagnostic of silicon carbide surge arresters of substation. WSEAS Transactions on Systems. Vol. 8, No. 12, (December 2009) 1284-1293, ISSN 1109-2777.

Kannus, K. & Lahti, K. (2005). Evaluation of the operational condition and reliability of surge arresters used on medium voltage networks. *IEEE Transactions on Power Delivery*, Vol. 20, No. 2, (April 2005) 745-750, ISSN 0885-8977.

McDermid, W. (2002). Reliability of station class surge arresters, *Proceedings of the 2002 IEEE International Symposium on Electrical Insulation*, pp. 320-322, ISBN 0-7803-7337-5, Boston, April 2002.

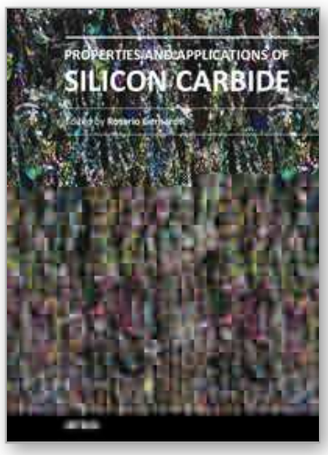

Properties and Applications of Silicon Carbide

Edited by Prof. Rosario Gerhardt

ISBN 978-953-307-201-2
Hard cover, 536 pages
Publisher InTech
Published online 04, April, 2011
Published in print edition April, 2011

In this book, we explore an eclectic mix of articles that highlight some new potential applications of SiC and different ways to achieve specific properties. Some articles describe well-established processing methods, while others highlight phase equilibria or machining methods. A resurgence of interest in the structural arena is evident, while new ways to utilize the interesting electromagnetic properties of SiC continue to increase.

How to reference

In order to correctly reference this scholarly work, feel free to copy and paste the following:

Arnaldo Gakiya Kanashiro and Milton Zanotti Jr. (2011). Contribution to the Evaluation of Silicon Carbide Surge Arresters, Properties and Applications of Silicon Carbide, Prof. Rosario Gerhardt (Ed.), ISBN: 978-953-307-201-2, InTech, Available from: http://www.intechopen.com/books/properties-and-applications-of-silicon-carbide/contribution-to-the-evaluation-of-silicon-carbide-surge-arresters

INTECH
open science | open minds

InTech Europe
University Campus STeP Ri
Slavka Krautzeka 83/A
51000 Rijeka, Croatia
Phone: +385 (51) 770 447
Fax: +385 (51) 686 166
www.intechopen.com

InTech China
Unit 405, Office Block, Hotel Equatorial Shanghai
No.65, Yan An Road (West), Shanghai, 200040, China
中国上海市延安西路65号上海国际贵都大饭店办公楼405单元
Phone: +86-21-62489820
Fax: +86-21-62489821

IntechOpen